Molecular Therapy
Nucleic Acids
Original Article

LINC00941 promotes glycolysis in pancreatic cancer by modulating the Hippo pathway

Ming Xu,[2,3] Ran Cui,[1,3] Lunhe Ye,[1,3] Yongkun Wang,[1] Xujing Wang,[1] Qiqi Zhang,[1] Kaijing Wang,[1] Chunxiu Dong,[1] Wenjun Le,[1] and Bo Chen[1]

[1]Department of Hepatopancreatobiliary Surgery, Translational Medical Center for Stem Cell Therapy, Shanghai East Hospital, School of Medicine, Tongji University, Shanghai 200123, China; [2]Department of Gastroenterology, Pudong New Area People's Hospital, Shanghai 201200, China

Pancreatic ductal adenocarcinoma (PDAC) is one of most lethal cancers and is projected to be the second leading cause of cancer deaths in the United States by 2030. The lack of effective treatment and increased incidence in PDAC encourage a deeper knowledge of PDAC progression. By analyzing a long noncoding RNA (lncRNA) dataset, we found that increased LINC00941 expression led to poor outcomes in PDAC patients. Furthermore, *in vitro* and *in vivo* experiments revealed that LINC00941 promoted PDAC cancer cell growth by enhancing aerobic glycolysis. Mechanistically, LINC00941 was found to interact with mammalian STE20-like protein kinase 1 (MST1), which facilitated the protein phosphatase 2A (PP2A)-mediated dephosphorylation of MST1, resulting in Hippo pathway activation and consequently, enhanced glycolysis in PDAC. These results suggest that LINC00941 plays a key role in regulating PDAC tumorigenesis, potentially highlighting novel avenues for PDAC therapy.

INTRODUCTION

Pancreatic cancer is a highly aggressive cancer and is projected to be the second leading cause of cancer-related death worldwide in 2030.[1,2] Although much effort has been made, the diagnosis and treatment methods for pancreatic ductal adenocarcinoma (PDAC) have not progressed much in recent decades. The overall 5-year survival rate of PDAC patients is still less than 8%.[3] Therefore, it is urgent to reveal the underlying mechanisms of PDAC progression and develop novel therapeutic targets for improving the survival of PDAC patients.

Recently, metabolic reprogramming has been identified as one of the hallmarks of cancer,[4] especially in PDAC.[5] To sustain rapid proliferation and provide building blocks for synthetic reactions, pancreatic cancer cells take up enormous amounts of glucose and ferment it to produce lactate even under sufficient oxygen conditions, which is called the Warburg effect.[6] An increasing number of studies have reported that many glycolytic enzymes are associated with the poor prognosis in PDAC,[7–9] indicating that disturbing glycolysis is a potential strategy to inhibit the tumorigenic activity of PDAC cells.

Owing to the development of high-throughput sequencing technologies, our knowledge of cancer transcriptomes is ever increasing. It is now evident that although less than 2% of the genome encodes proteins, at least 75% is actively transcribed into noncoding RNAs.[10] Most of these noncoding transcripts surpass 200 nucleotides in length, also called long noncoding RNAs (lncRNAs).[11] Increasing evidence has indicated that lncRNAs play crucial roles in various biological processes, including apoptosis,[12] proliferation,[13,14] and stem cell-like processes.[15] However, the role of lncRNA-mediated metabolic reprogramming in PDAC remains largely unclear. Previous studies have demonstrated that lncRNAs are associated with PDAC.[16–18] In this study, we found a series of lncRNAs that were aberrantly expressed in PDAC by analyzing a published lncRNA microarray dataset. Specifically, we found that increased LINC00941, also named lncRNA-MUF, expression was associated with poor prognosis in pancreatic cancer. Furthermore, functional experiments revealed that LINC00941 promotes PDAC cancer cell growth by enhancing aerobic glycolysis. Moreover, RNA-binding protein immunoprecipitation (RIP) and RNA pull-down experiments validated an interaction between LINC00941 and mammalian STE20-like protein kinase 1 (MST1), which facilitates the protein phosphatase 2A (PP2A)-mediated dephosphorylation of MST1, resulting in Hippo pathway activation and consequently, enhanced glycolysis in PDAC. Taken together, these results provide evidence that LINC00941 may serve as a novel potential therapeutic target for PDAC.

RESULTS

Increased LINC00941 expression is positively correlated with disease progression and poor prognosis in PDAC

First, we compared lncRNA expression across pancreatic cancer and paired adjacent nontumor pancreatic tissue samples and found that compared to nontransformed pancreatic tissues, 34 lncRNAs were significantly upregulated, and 32 lncRNAs were downregulated in

Received 1 December 2020; accepted 7 July 2021;
https://doi.org/10.1016/j.omtn.2021.07.004.

[3]These authors contributed equally

Correspondence: Bo Chen, Department of Hepatopancreatobiliary Surgery, Translational Medical Center for Stem Cell Therapy, Shanghai East Hospital, School of Medicine, Tongji University, 1800 Yuntai Road, Shanghai 200123, China
E-mail: chenbo7349@sohu.com
Correspondence: Wenjun Le, Department of Hepatopancreatobiliary Surgery, Translational Medical Center for Stem Cell Therapy, Shanghai East Hospital, School of Medicine, Tongji University, 1800 Yuntai Road, Shanghai 200123, China
E-mail: wenjunle@tongji.edu.cn

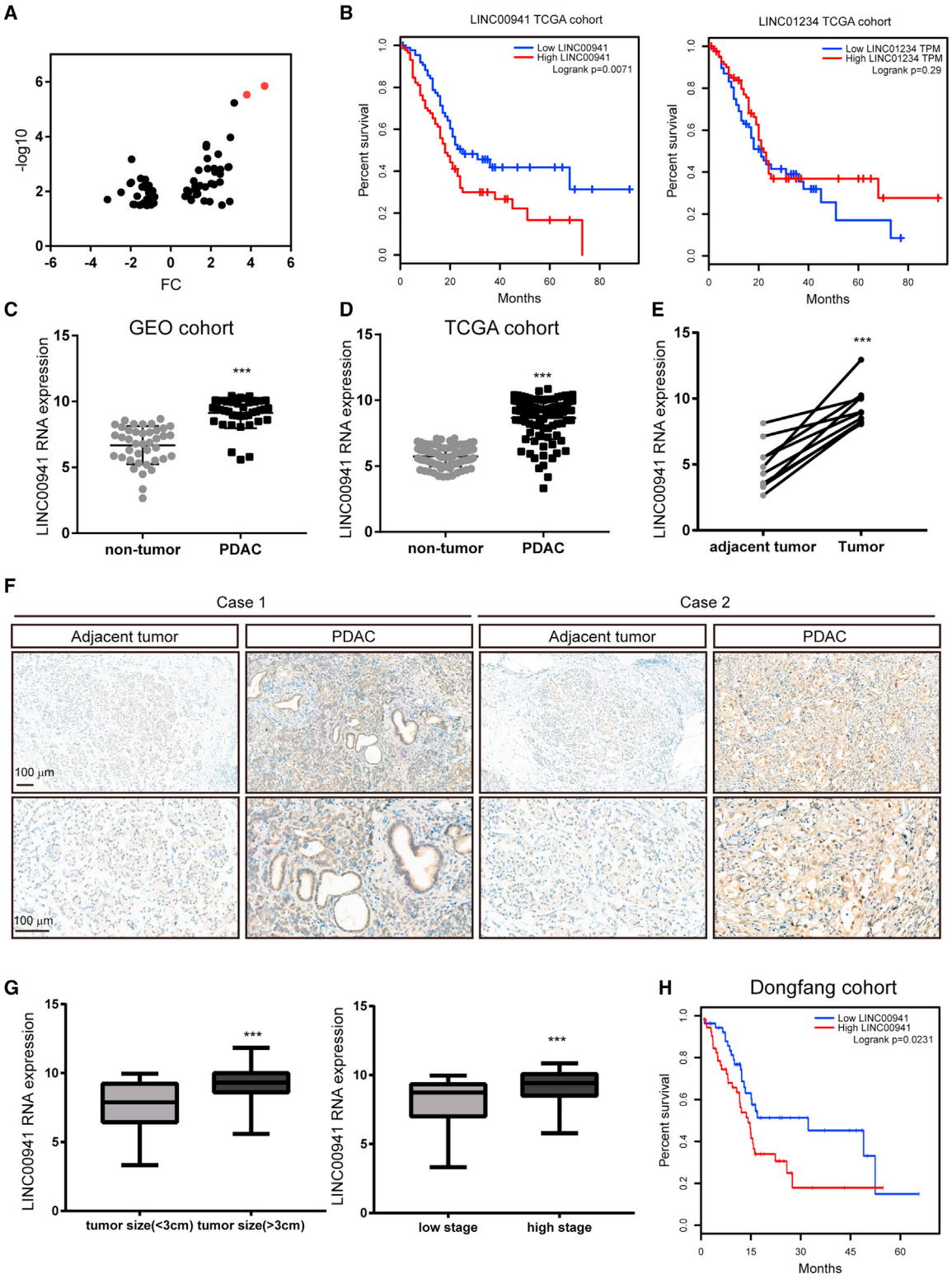

(legend on next page)

pancreatic cancer tissues (Figure 1A). We next analyzed the correlation of the top two upregulated lncRNAs, LINC00941 and LINC01234, with clinical outcome in The Cancer Genome Atlas (TCGA) dataset. The Kaplan-Meier analysis results showed that LINC01234 had no predictive value for the overall survival of pancreatic cancer patients, but LINC00941 was significantly associated with poor prognosis in these patients (Figure 1B). In line with datasets from the Gene Expression Omnibus (GEO), we found that LINC00941 was highly expressed in the PDAC TCGA dataset compared to normal pancreas Genotype-Tissue Expression (GTEx) datasets (Figures 1C and 1D). To confirm the microarray data, LINC00941 expression was detected in 10 cases of paired pancreatic cancer and adjacent tissues by real-time PCR. Consistently, we found that LINC00941 expression was dramatically increased in PDAC tissues (Figure 1E). Furthermore, we validated LINC00941 expression via *in situ* hybridization (ISH) in paraffin-embedded pancreatic cancer and adjacent tissues. The results showed that LINC00941 was mainly localized to the cytosol of PDAC cells, and, LINC00941 expression was higher in pancreatic cancer tissues than in adjacent tissues (Figures 1F and S1). Next, we assessed the correlation of LINC00941 expression with different clinic-pathological features in TCGA dataset. We found that LINC00941 expression positively correlated with tumor size and tumor stage (Figure 1G). Consistent with the results in TCGA cohort, high levels of LINC00941 expression were significantly associated with a shortened survival time in PDAC patients.

LINC00941 depletion suppresses PDAC cancer cell growth *in vitro*

To reveal the function of LINC00941 in pancreatic cancer progression, we used a lentiviral vector-based short hairpin (sh)RNA system to silence the expression of LINC00941 in two PDAC cancer cell lines expressing high levels of LINC00941: PANC-1 and SW1990 (Figure 2A). The shRNA of LINC00941 dramatically suppressed the LINC00941 expression in PDAC cell lines (Figure 2B). Cell viability assays showed that the loss of LINC00941 greatly inhibited the proliferation of PANC-1 and SW1990 cells (Figure 2C). In contrast, LINC00941 overexpression significantly promoted the growth of BxPC-3 and CFPAC-1 cells, two PDAC cancer cells with relatively low LINC00941 expression (Figures 2D and S2). Consistently, a colony formation assay showed that knockdown of LINC00941 significantly suppressed the colony formation ability of PDAC cancer cells (Figure 2E). To further mimic the growth conditions *in vivo*, 3D growth experiments were employed to compare the growth ability of LINC00941-silenced PDAC cells and control cells. In line with 2D culture, loss of LINC00941 significantly inhibited the sphere growth of PDAC cell lines (Figure 2F). Collectively, the data suggest that inhibition of LINC00941 impairs the growth of PDAC cancer cells.

LINC00941 depletion inhibits glycolysis in PDAC cells

Next, we aimed to elucidate the mechanism by which LINC00941 regulates the growth of PDAC cancer cells. Interestingly, we observed that when cultured in fresh medium for 12 h to the same confluence, the phenol red in the control PDAC cell culture medium exhibited a gradual color transition from red to yellow, whereas LINC00941-silenced tumor cell lines failed to exhibit this color shift (Figure 3A). These results suggest that LINC00941 suppresses extracellular acidic production. The measurement of the extracellular pH of culture medium confirmed that the culture medium derived from control tumor cells gradually became more acidic, whereas the culture medium from LINC00941-silenced tumor cell lines did not become acidic as quickly as that from control cells (Figure 3B). To precisely compare the extracellular acidification rate (ECAR) of control cells and LINC00941-silenced cells, an ECAR kit was employed using a Seahorse XF96 analyzer. Indeed, knockdown of LINC00941 dramatically suppressed the glycolysis ability of both PANC-1 and SW1990 cells (Figures 3C and 3D). Thus, we measured the mRNA expression level of enzymes in the glycolysis pathway. We found that glucose transporter type 1 (*GLUT1*), hexokinase 2 (*HK2*), *PFKFB3*, and lactate dehydrogenase A (*LDHA*) mRNA expression was greatly reduced upon the silencing of LINC00941(Figures 3E and 3F). In addition, we compared the glucose uptake and lactate production of LINC00941 sh-negative control (shNC), sh1, and sh2 PDAC cells. As expected, knockdown of LINC00941 significantly suppressed the glucose uptake and lactate production of PDAC cancer cells (Figures 3G and 3H). Taken together, these data revealed that loss of LINC00941 inhibits glycolysis in PDAC cells.

Glycolysis is necessary for LINC00941-mediated growth promotion

Next, we aimed to evaluate whether the enhanced glycolysis is necessary for LINC00941-mediated growth-promoting effects in PDAC cells. Thus, we first blocked glycolysis in BxPC-3 and CFPAC-1 cells ectopically expressing LINC00941 with the hexokinase 2-specific inhibitor 2-deoxyglucose (2-DG) for 24 h. Cell proliferation assay results showed that 2-DG administration greatly impaired the growth-promoting effects induced by LINC00941 overexpression in BxPC-3 and CFPAC-1 cells (Figures 4A and 4B). To further confirm this, the glucose in the culture medium was replaced with galactose to inhibit glycolysis. As expected, lactate production was dramatically reduced upon galactose replacement. Consistently, the proliferation of BxPC-3 and CFPAC-1 cells ectopically expressing LINC00941 sharply decreased (Figures 4C and 4D). To further confirm this in

Figure 1. High LINC00941 associated poor prognosis in PDAC patients

(A) The dysregulated expression of lncRNAs in PDAC tissues. (B) Kaplan-Meier analysis of the correlation of LINC00941 and LINC01234 in TCGA PDAC cohort. The median of LINC00941 or LINC01234 expression was used to distinguish the high and low lncRNA group. (C–E) The expression of LINC00941 in the GEO dataset cohort (C), TCGA and GTEx (D), and dongfang cohort (E). (F) *In situ* hybridization (ISH) of LINC00941 in PDAC tumor adjacent and tumor tissues. (G) The comparison of LINC00941 expression in different tumor size and tumor stages. (H) Kaplan-Meier analysis of the correlation of LINC00941 in the dongfang PDAC cohort. (C–E and G) Statistical significances were calculated using two-tailed Student's t tests. (B and H) Statistical significances were calculated using log-rank Cox test. *$p < 0.05$; **$p < 0.01$; ***$p < 0.001$.

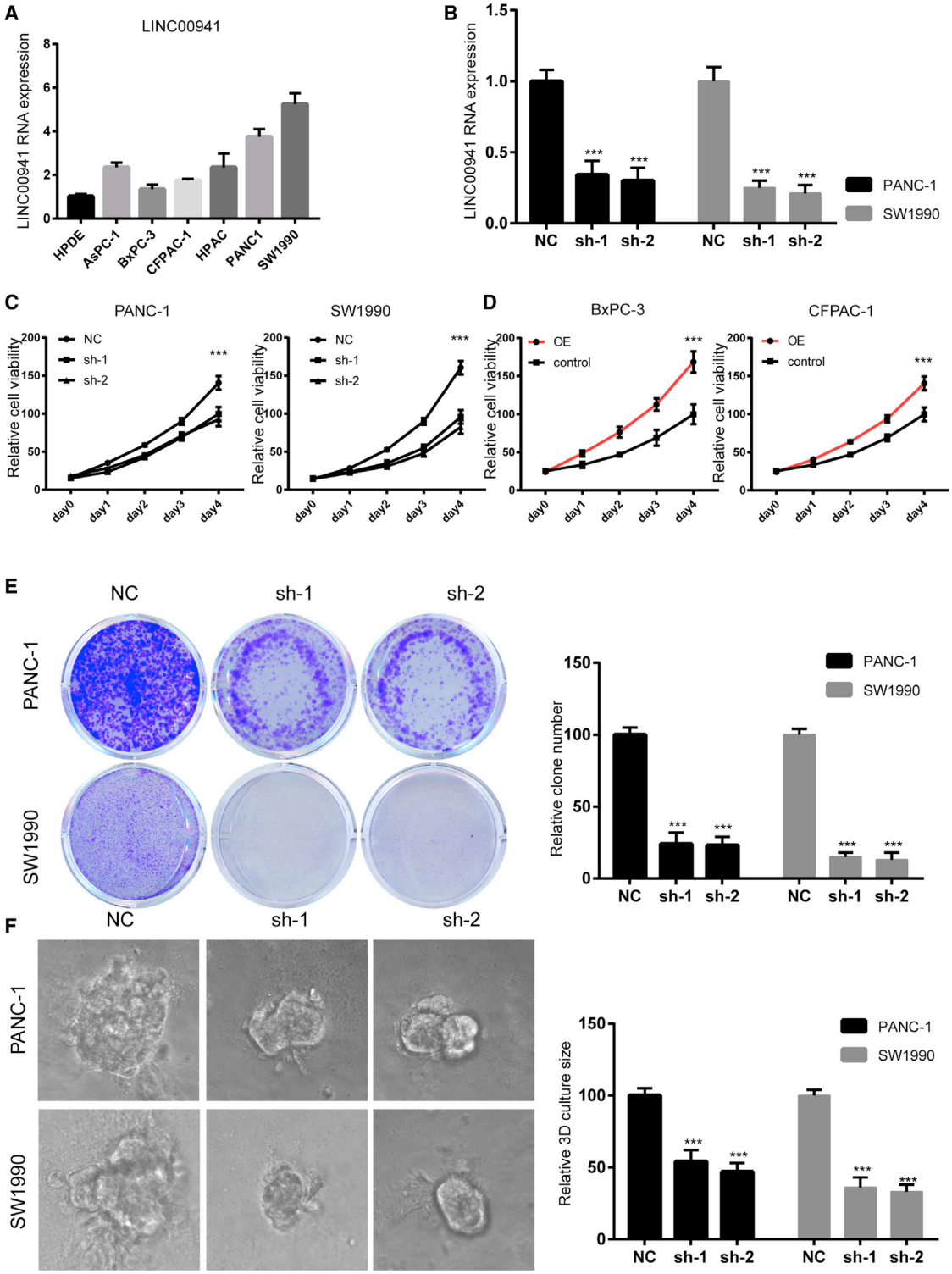

Figure 2. LINC00941 depletion suppresses the growth of PDAC cancer cells

(A) LINC00941 expression in human pancreatic duct epithelial (HPDE) and PDAC cancer cell lines. (B) Knockdown efficiency in PANC-1 and SW1990 cells. (C and D) Cell viability assay of PDAC cell lines silenced with LINC00941 or overexpressed with LINC00941. (E) Represented results of the colony formation in LINC00941 control and knockdown cell lines. (F) Represented results of the 3D-on-top growth in LINC00941 control and knockdown cell lines. All statistical significances were calculated using two-tailed Student's t tests to compare with the NC or control group. *$p < 0.05$; **$p < 0.01$; ***$p < 0.001$.

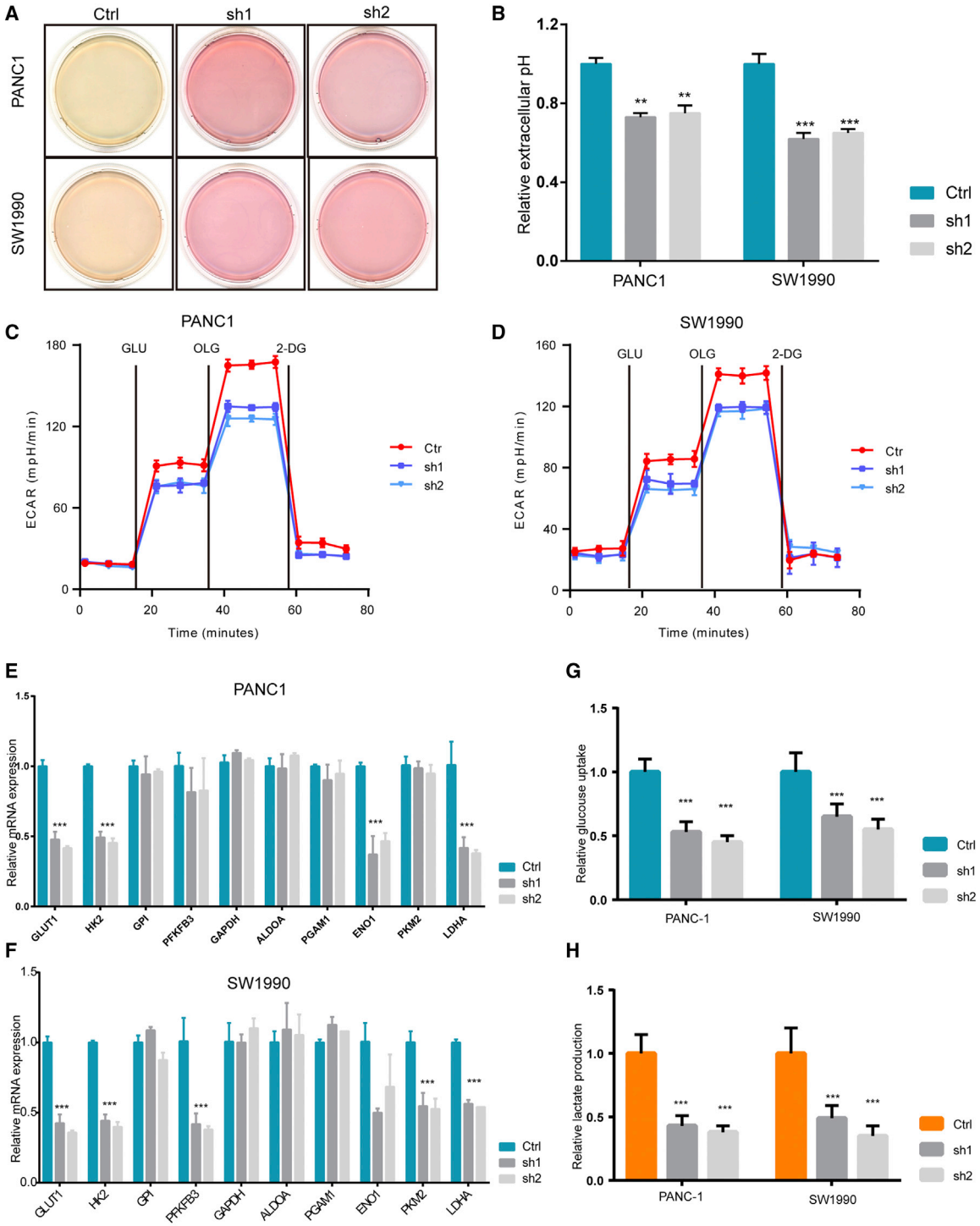

Figure 3. Loss of LINC00941 inhibited the glycolysis of PDAC cancer cells

(A) Representative culture plate scan results of PDAC control or LINC00941 knockdown cells. (B) Relative extracellular pH of PDAC control or LINC00941 knockdown cells. (C and D) ECAR analysis of control or LINC00941 knockdown of PANC-1 (C) and SW1990 (D) cells. (E and F) qPCR results of genes related to the glycolysis process in PANC-1 and SW1990 cells. (G) Glucose uptake of PDAC cell lines with indicated treatment. (H) Lactate production of PDAC cell lines with indicated treatment. All statistical significances were calculated using two-tailed Student's t tests to compare with the NC or control group. *$p < 0.05$; **$p < 0.01$; ***$p < 0.001$.

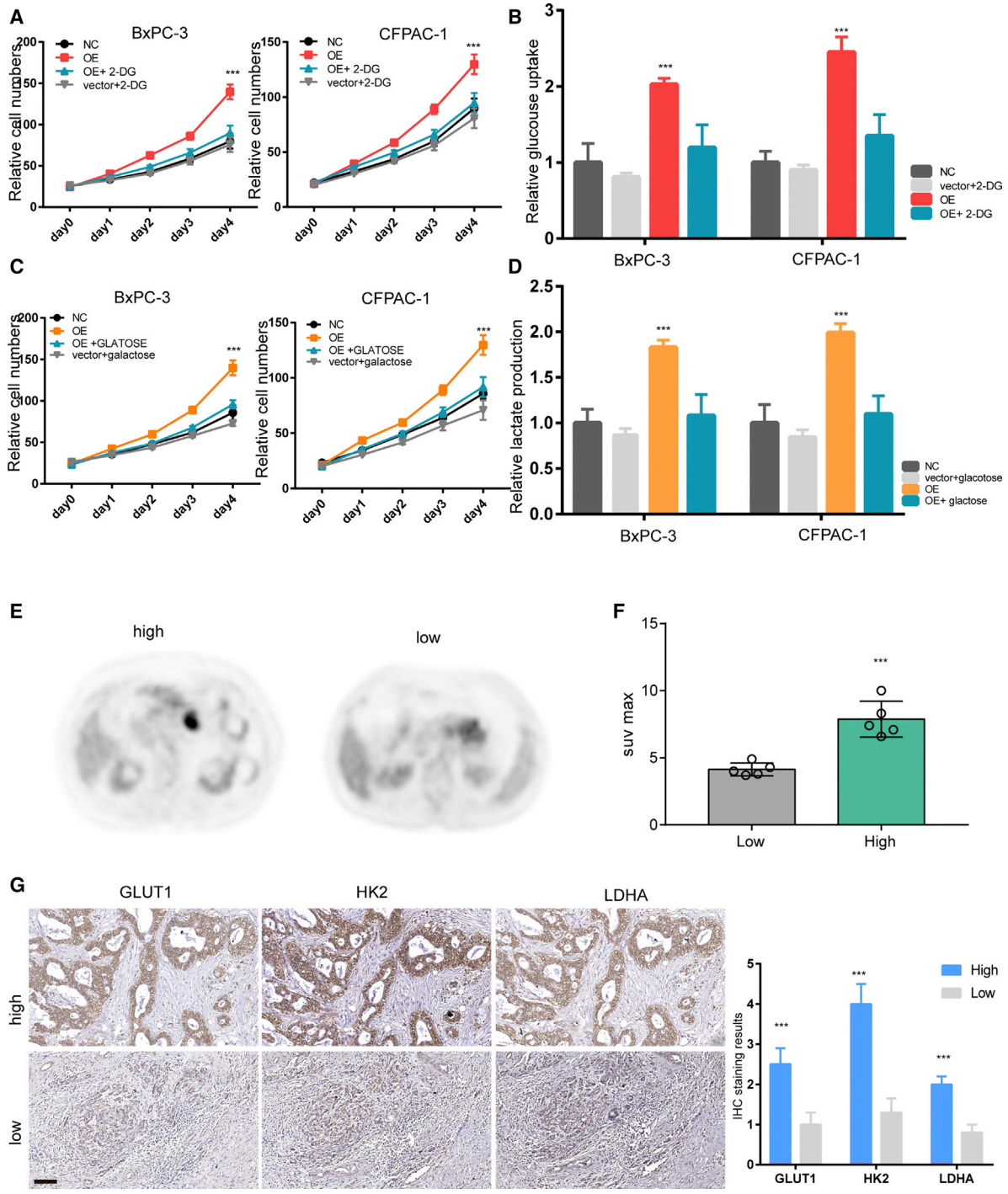

Figure 4. Growth-promoting effects of LINC00941 to PDAC cells depend on the enhanced glycolysis

(A) Cell viability assay of PDAC cell lines with LINC00941 overexpression and 2-DG treatment or not. (B) Glucose uptake of PDAC cell lines with LINC00941 overexpression and 2-DG treatment or not. (C) Cell viability assay of PDAC cell lines with indicated treatment cultured in medium in which galactose replaced glucose. (D) Lactate production of PDAC cell lines with indicated treatment cultured in medium in which galactose replaced glucose. (E) Representative PET-CT results of high and low LINC00941 expression of PDAC patients. (F) The SUVmax statistical results of PDAC patients. (G) IHC staining of high and low LINC00941 expression of PDAC specimens. All statistical significances were calculated using two-tailed Student's t tests to compare with the NC or control group. *$p < 0.05$; **$p < 0.01$; ***$p < 0.001$.

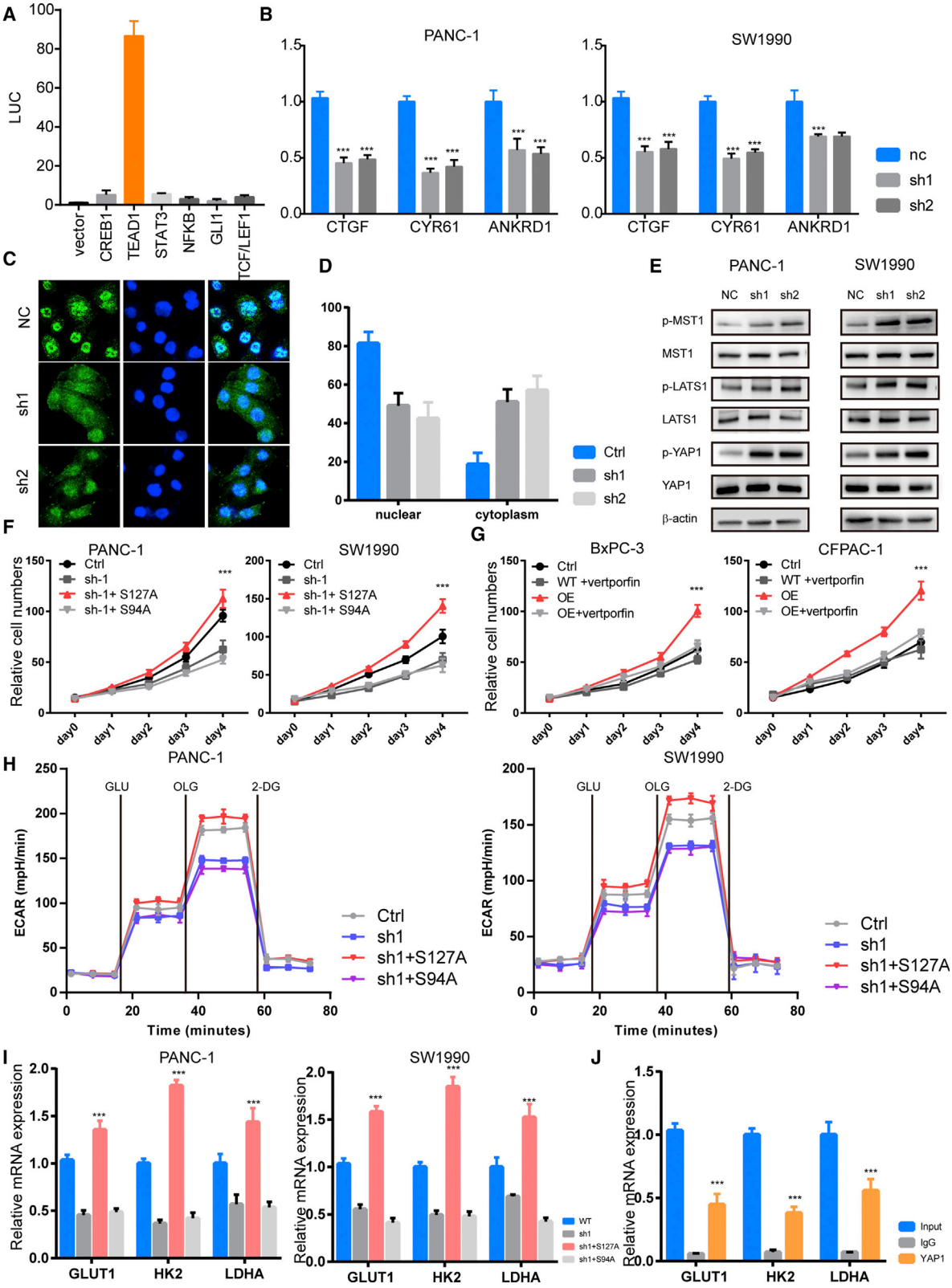

(legend on next page)

PDAC specimens, ten pancreatic cancer samples with positron emission tomography-computed tomography (PET-CT) data were divided into two groups according to LINC00941 expression: the LINC00941 low group and the LINC00941 high group (Figures 4E and 4F). Further comparison showed that the LINC00941 high group exhibited a higher maximum standardized uptake value (SUVmax) value and stronger GLUT1, HK2, PFKFB3, and LDHA staining than the LINC00941 low group (Figures 4E–4G). Collectively, these data suggest that glycolysis is necessary for LINC00941-mediated growth-promoting effects.

LINC00941 activates the Hippo pathway to enhance glycolysis in PDAC cells

Further, we aimed to reveal the signaling pathway by which LINC00941 enhances glycolysis in PDAC cells. Several transcriptional factors that have been reported to regulate glycolysis—cyclic AMP (cAMP)-responsive element-binding protein (CREB), TEA domain transcription factor 1 (TEAD1), GLI family zinc finger 1 (GLI1), and transcription factor (TCF)/lymphoid enhancer binding factor 1 (LEF1)—were studied by luciferase reporter assays.[19–23] We found that transfection of LINC00941 markedly increased the transcriptional activity of TEAD1 but not the other transcription factors in PANC-1 cells (Figure 5A), and knockdown of LINC00941 reduced the transcriptional activity of TEAD 1 (Figure S3), indicating that the Hippo pathway may mediate the regulation of glycolysis by LINC00941. Thus, we detected the expression of three typical downstream genes of the Hippo pathway: *CTGF*, *CYR61*, and *ANKRD1*. The results showed that LINC00941 knockdown greatly reduced the mRNA expression levels of these three target genes in both PANC-1 and SW1990 PDAC cells (Figure 5B). To further confirm this, the subcellular location of Yes1 associated transcriptional regulator (YAP1) in control and LINC00941-silenced PDAC cells was detected by immunofluorescence staining. We found that the proportion of YAP1 with nuclear localization was much higher in LINC00941 sh1 and sh2 PANC-1 cells than in control cells (Figures 5C and 5D). Next, immunoblotting was performed to detect alterations in the Hippo pathway in LINC00941-silenced PDAC cell lines. The results showed that phosphorylation levels of MST1, large tumor suppressor kinase 1 (LATS1), and YAP1 were obviously upregulated in LINC00941 knockdown cells compared to control cells (Figure 5E). To further determine whether YAP1 is necessary for the oncogenic role of LINC00941 in PDAC, two YAP1 mutants were introduced into LINC00941-overexpressing or LINC00941-depleted PDAC cells. As expected, ectopic expression of the constitutively activated form YAP1 (S127A) reversed the impaired growth of LINC00941-depleted PDAC cells. Conversely, ectopic expression of loss of function YAP1 (S94A) did not hinder the growth-promoting effects mediated by LINC00941 overexpression (Figures 5F and S4). Similarly, verteporfin, an inhibitor of Hippo pathway, impedes the growth of LINC00941-overexpressing cells (Figure 5G). In addition, ECAR measurement results showed that YAP1 (S127A) overexpression restored the impaired glycolysis in LINC00941-depleted PDAC cells and that YAP1 (S94A) overexpression impeded the glycolysis enhancement mediated by LINC00941 overexpression (Figure 5H). Thus, we hypothesized that YAP1 could transactivate the expression of glycolysis enzymes. The real-time PCR results showed that the YAP1 S127A mutant could reverse the expression of *GLUT1*, *HK2*, *PFKFB3*, and *LDHA* in LINC00941 knockdown PDAC cells, but the YAP1 S94A mutant could not (Figure 5I). Furthermore, the chromatin immunoprecipitation (ChIP)-PCR results showed that YAP1 could directly bind to the promoters of the *GLUT1*, *HK2*, *PFKFB3*, and *LDHA* genes. Collectively, these data suggest that the Hippo pathway is a mediator of the enhanced glycolysis induced by LINC00941.

LINC00941 facilitates the PP2A-mediated dephosphorylation of MST1 to trigger the Hippo pathway

To elucidate the mechanism by which LINC00941 activates the Hippo pathway, we first determined the subcellular localization of LINC00941 in PDAC cells. The ISH staining results showed that LINC00941 was mainly localized to the cytosol of PDAC cells (Figure 6A). Furthermore, LINC00941 RNA pull-down followed by mass spectrometry analysis was performed to screen for potential proteins interacting with LINC00941 (Figure 6B). The results showed that MST1, one of the key nodes of the Hippo pathway, could interact with LINC00941. In line with this, immunoblotting data showed that LINC00941, but not antisense LINC00941, could interact with MST1 (Figure 6C). To further confirm this interaction, a RIP assay was performed in PANC-1 cell lines. As expected, LINC00941 could be detected in the MST1 precipitate but not the immunoglobulin G (IgG) precipitate by both gel electrophoresis and qPCR assays (Figures 6D and 6E). To clarify the exact regions of LINC00941 and MST1 that interact, we constructed a series of truncated LINC00941 variants. Nucleotides 800 to 1,500 of LINC00941 were found to bind MST1 (Figure 6F). As expected, overexpressing (truncated LINC00941 depletion nucleotide 800−1500 [Δ] 800−1,500) LINC00941 could not promote the proliferation and glycolysis as well as wild-type (WT) LINC00941 in PDAC cell (Figures S5A and S5B). Competitive RNA pull-down assays and MST1 and LINC00941immunofluorescence staining further confirmed the interaction of LINC00941 with MST1 (Figures 6G and 6H). With the consideration that LINC00941 knockdown results in an increase

Figure 5. LINC00941 enhances the glycolysis of PDAC cells via the Hippo pathway

(A) Luciferase report assays of pathways that reported involvement in cancer cell glycolysis. (B) qPCR results of Hippo pathway target genes upon LINC00941 knockdown. (C) Immunofluorescence staining of Yes1 associated transcriptional regulator (YAP1) in control and LINC00941 knockdown of PANC-1 cells. (D) Statistical results of YAP1 immunofluorescence staining. (E) Immunoblots of the Hippo pathway in control and LINC00941 knockdown PDAC cells. (F and G) Cell viability assay of PDAC cells transfected with mutant YAP1 (F) and LINC00941 plus verteporfin treatment. (H) ECAR assay of PDAC cells transfected with mutant YAP1. (I) qPCR results of glycolysis-altered genes in PDAC cells transfected with mutant YAP1. (J) ChIP-PCR results of YAP1 in PANC-1 cells. All statistical significances were calculated using two-tailed Student's t tests to compare with the NC or control group. *$p < 0.05$; **$p < 0.01$; ***$p < 0.001$.

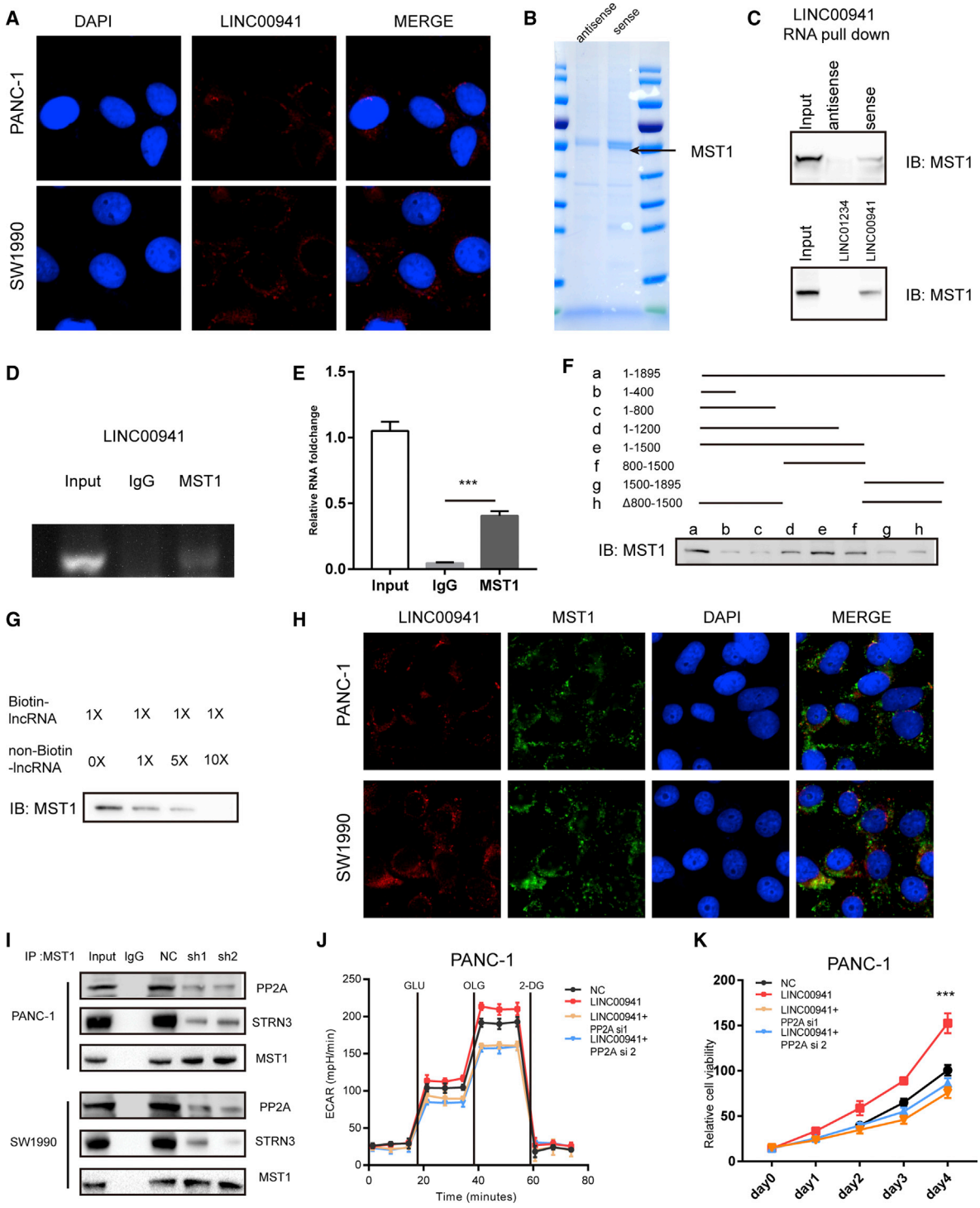

Figure 6. LINC00941 interacted with mammalian STE20-like protein kinase 1 (MST1) to trigger the Hippo pathway

(A) ISH fluorescence staining of LINC00941. (B) RNA pull-down assay with LINC00941, followed by Coomassie staining. (C) RNA pull-down assay with LINC00941 and LINC01234, followed by MST1 immunoblots. (D and E) RNA-binding protein immunoprecipitation (RIP) assay for MST1, followed by LINC00941 agarose gel electrophoresis and qPCR (E). (F) RNA pull-down assay for full-length or truncated LINC00941, followed by immunoblots using the MST1 antibody. (G) Competition assays using

(legend continued on next page)

in MST1 phosphorylation, we hypothesize that LINC00941 may mediate the dephosphorylation of MST1. Previous studies showed that MST1 dephosphorylation was mediated by PP2A;[24] thus, we detected the interaction of MST1 and PP2A upon LINC00941 silencing. The co-immunoprecipitation (coIP) results showed that the interaction between MST1 and PP2A was weaker in LINC00941-silenced cells than control cells and also the striatin 3 (STRN3), which was reported to bind to MST1 and PP2A[24] (Figures 6I, S5C, and S5D). We further confirmed whether PP2A is involved in LINC00941-mediated Hippo activation. After PP2A was silenced by small interfering RNA (siRNA), a luciferase reporter assay was performed. We found that knockdown of PP2A markedly impeded the enhanced TEAD1 transcriptional activity-mediated LINC00941 overexpression by both BXPC-3 and CFPAC-1 PDAC cells (Figure S6A). As expected, PP2A silencing counteracted the enhanced glycolysis and growth-promoting effects in BXPC-3 and CFPAC-1 cells (Figures 6J, 6K, S6B, and S6C). Together, these results suggest that LINC00941 facilitates the PP2A-mediated dephosphorylation of MST1 to trigger the Hippo pathway.

Targeting LINC00941 impedes the progression of PDAC *in vivo*

We next evaluated whether LINC00941 loss disturbs the formation of PDAC *in vivo*. First, control and shLINC00941 PANC-1 cells were inoculated subcutaneously into nude mice to generate a subcutaneous xenograft model. The results showed that control cell-injected mice developed larger tumors than that in LINC00941 knockdown cell-injected mice (Figure 7A). Statistical analysis of the tumor volumes (Vs) indicated that the subcutaneous xenografts derived from control cells developed much more rapidly than those derived from shLINC00941 cells (Figure 7B). Consistently, according to tumor weight, the tumor burden in shLINC00941 cell-injected mice was less than that in control cell-injected mice (Figure 7C). Indeed, the immunohistochemistry (IHC) staining analysis of resected tumor sections revealed that tumors derived from shLINC00941 cells exhibited weaker proliferating cell nuclear antigen (PCNA), YAP1, GLUT1, HK2, and LDHA staining than those derived from shNC cells (Figure 7D). Furthermore, we transplanted 1×10^6 luciferase-expressing shNC or shLINC00941 cells into the pancreas of nude mice and subsequently performed bioluminescence imaging every 5 days to monitor the development of orthotopic tumors. The *in vivo* imaging system (IVIS) results revealed that LINC00941 loss reduced the aggressiveness of PDAC cells (Figure 7E) and prolonged the overall survival of orthotopic xenograft mice (Figure 7F). To determine potential synergistic effects with first-line drugs, gemcitabine (50 mg/kg) was administered to implanted mice every 5 days. The results showed that the mice in the shLINC00941 plus gemcitabine group developed smaller tumors and had longer overall survival than those with LINC00941 depletion or gemcitabine treatment alone (Figure 7F). As expected, sections from mice in the shLINC00941 plus gemcitabine group exhibited weaker PCNA, YAP1, GLUT1, HK2, and LDHA staining than those with LINC00941 depletion or gemcitabine treatment alone (Figure 7G). Thus, loss of LINC00941 decreases tumor burden and attenuates PDAC progression *in vivo*.

DISCUSSION

Here, we identified that LINC00941 was highly expressed in PDAC, which was closely associated with poor prognosis in patients with PDAC. Depletion of LINC00941 greatly suppresses PDAC cancer cell growth by inhibiting aerobic glycolysis. Our mechanistic study revealed that LINC00941 could interact with MST1, which facilitates the dephosphorylation MST1 by PP2A, resulting in Hippo pathway activation and subsequent enhancement of glycolysis in PDAC. In this study, we revealed the role and mechanism of LINC00941 as a pioneering factor enhancing the Hippo pathway and promoting the progression of PDAC.

LINC00941 is a recently identified lncRNA found to facilitate tumorigenesis.[25] Previous studies have reported that LINC00941 triggers Wnt/β-catenin signaling and promotes the epithelial-mesenchymal transition of liver cancer cells and gastric cancer cells.[25–27] Upregulation of LINC00941 activates the phosphatidylinositol 3-kinase (PI3K)-AKT serine/threonine kinase (AKT) signaling pathway in lung cancer.[28] Also, LINC00941 promotes invasiveness by restraining cell proliferation and autophagy in thyroid cancer.[29] Additionally, Nan Wu et al.[30] reported that LINC00941 promotes the metastasis of colorectal cancer (CRC) by activating the transforming growth factor (TGF)-β/mothers against decapentaplegic homolog (SMAD)2/3 signaling pathway by preventing SMAD4 protein degradation. In our study, we found that depletion of LINC00941 dramatically suppressed glycolysis in PDAC cancer cells and that overexpression of LINC00941 in cancer cells with low LINC00941 expression enhanced glycolysis, indicating that LINC00941 acts as a positive regulator of glycolysis in PDAC. Consistently, LINC00941 silencing was found to lead to glycolysis-related enzyme expression deregulation. In addition, inhibition of glycolysis by 2-DG or glycolysis deprivation significantly impeded the pro-tumorigenic effects of LINC00941, suggesting that the growth-promoting effects of LINC00941 depend on its regulation of glycolysis. Combined with previous studies and our study, LINC00941 presents a variety of function in different cancer types, which may be owing to the genetic difference in different cancer type or the diversity of protein that interacted with LINC00941 in cancer cells, and, more efforts were needed to completely understand the roles in different cancer progression.

Given that glycolysis is essential for LINC00941-induced cancer cell growth, we next focused on the relationship between LINC00941 and glycolysis. Our data revealed that LINC00941 could interact

biotin-labeled and unlabeled LINC00941. (H) Immunofluorescence staining of MST1 and LINC00941. (I) CoIP assays were performed with MST1 antibody in LINC00941 control and knockdown cells, followed by PP2A, striatin 3 (STRN3), and MST1 detection by WB. (J) ECAR analysis of control or PP2A knockdown PANC-1. (K) Cell viability assay of control or PP2A knockdown PANC-1. All statistical significances were calculated using two-tailed Student's t tests to compare with the NC or control group. *$p < 0.05$; **$p < 0.01$; ***$p < 0.001$.

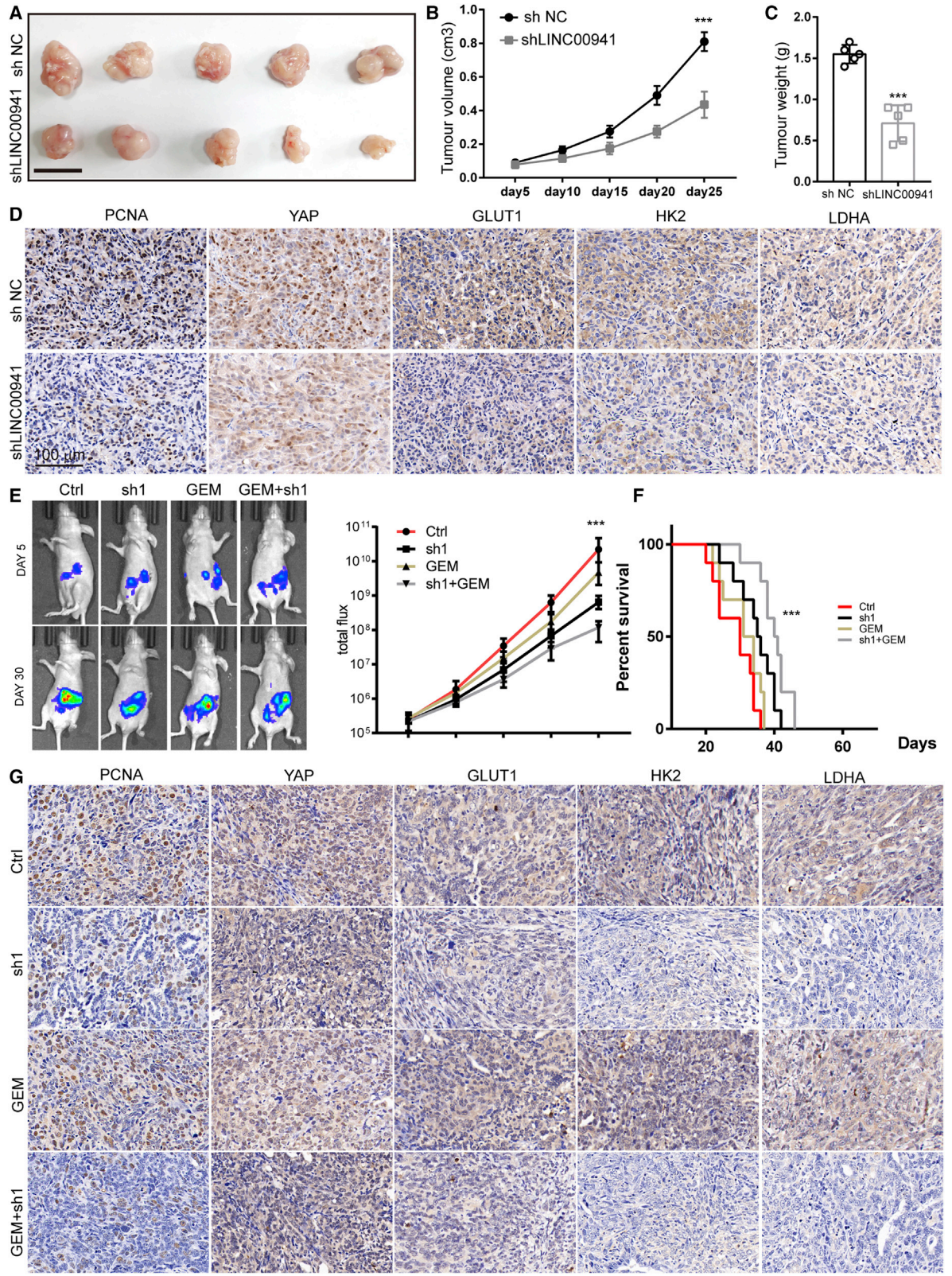

(legend on next page)

with MST1, which is a key node of the Hippo pathway.[31] Further, LINC00941 loss-of-function experiments showed that LINC00941 depletion could inhibit the Hippo pathway. In line with our observations, Zheng et al.[32] reported that the Hippo pathway promotes glycolysis in breast cancer cell lines. The results of that study showed that YAP1 enhanced GLUT3 transcription. In our study, we found that YAP1 could promote the expression of GLUT1, HK2, and LDHA. In addition, YAP1 was reported to interact with hypoxia-inducible factor 1-alpha (HIF-1α) to sustain HIF-1α protein stability in hepatocellular carcinoma (HCC) cancer cells to promote glycolysis under hypoxic conditions.[33] Our data indicate that the Hippo pathway can also facilitate cancer cell glycolysis in PDAC.

Recently, accumulating evidence has shown that lncRNAs are involved in Hippo signaling regulation. The lncRNA uc.134 was reported to inhibit the Hippo pathway by inhibiting the cullin 4A (CUL4A)-mediated ubiquitination of LATS1 in HCC.[34] In papillary thyroid carcinoma, the lncRNA small nucleolar RNA host gene 15 (SNHG15) has been reported to act as a competing endogenous (ce)RNA to regulate YAP1 expression.[35] The lncRNA MNX1 antisense RNA 1 (MAYA) was reported to form a protein complex with Erb-B2 receptor tyrosine kinase 3 (HER3) and LLGL scribble cell polarity complex component 2 (LLGL2) to methylate MST1 at Lys59, leading to MST1 inactivation and activation of YAP target genes in breast cancer cells.[36] In our results, we found that LINC00941 could interact with MST1 and facilitate the dephosphorylation of MST1 by PP2A, resulting in increased YAP1 nuclear localization in PDAC cells. Additionally, STRN3 has been reported to be an essential regulatory subunit of PP2A that recruits and promotes the dephosphorylation of MST1/2 in gastric cancer.[24] Whether STRN3 is necessary for LINC00941-induced MST1 dephosphorylation remains to be determined.

In summary, our study revealed that high LINC00941 expression is positively associated with poor prognosis in PDAC. Loss-of-function and gain-of-function experiments showed that LINC00941 promotes growth and glycolysis of PDAC cancer cells. Mechanistic studies indicated that LINC00941 promotes YAP1 nuclear localization and downstream glycolysis-related gene expression by facilitating MST1 dephosphorylation. Furthermore, *in vivo* studies showed that LINC00941 deletion suppresses PDAC progression. Taken together, the results of our study reveal the protumor role and mechanism of LINC00941 in PDAC. Future efforts will attempt to evaluate its potential for therapy applications.

MATERIALS AND METHODS

Cell culture and regents

Human pancreatic cancer cell lines are obtained from the American Type Culture Collections (ATCC). All pancreas cancer cells (PANC-1, SW1990, CFPAC-1, and BxPC-3) were cultured in DMEM + 10% fetal bovine serum (FBS) and maintained at 37°C in a humidified atmosphere of 95% air and 5% CO_2. PANC-1 and SW1990 were selected to silence LINC00941 expression. Cell lines were routinely verified to be negative for mycoplasma by PCR.

RNA extraction and real-time PCR analyses

The total RNA of cancer cell lines was extracted by using TRIzol (TaKaRa; T9108), following reverse transcription using a PrimeScript RT Reagent Kit (TaKaRa; RR047A). The cDNA was mixed with SYBR Green mix (Roche; 4913914001), along with primers specific to Glut1, HK2, PFKFB3, ENO1, PFKFB3, PKM2, LDHA, and 18S, which were provided in Table S1. The relative expression level was calculated relative to the indicated control by using ΔCT (ΔCT(test) = CT(target, test) – CT(ref, test)) method.

Cell proliferation and colony formation assay

Cell proliferation assay was conducted by using a Cell Counting Kit 8 (CCK-8) Kit (Dojindo Laboratories), according to the manufacturer's guidelines. Briefly, cells were seeded into 96-well plates at a density of 3,000/well, following CCK-8 reagent incubated at 37°C for 1 h. The absorbance at 450 nm was used to determine the growth rate of cells. For colony formation assay, cells were seeded into 6-well plates at a density of 3,000/well, following 2 weeks' culture. Then the colony was fixed with 4% paraformaldehyde (PFA) for 15 min and stained with 3% crystal violet solution for 3 h. The experiments were performed in a quintuple manner and repeated twice. Images of colonies were captured and counted by using ImageJ.

3D culture

The 3D culture of tumor cells was performed according standard procedure. Briefly, cells were plated on 24-well ultra-low attachment plates (Corning) in complete media supplemented with 4% Matrigel (Corning). Media were refreshed every 4 days by carefully aspirating 50% of the well volume and replacing it with fresh complete media containing 1% Matrigel. The experiments were repeated twice.

Seahorse assay

ECAR and oxygen consumption rate (OCR) in this study were performed according to the manufacturer's instructions. Briefly, cells were

Figure 7. LINC00941 depletion inhibits PDAC growth *in vivo*

(A) Subcutaneous xenografts transplanted with PANC-1 control and LINC00941 knockdown cells (n = 5). Scale bar, 1 cm. (B) Tumor growth curve of subcutaneous xenografts. (C) Tumor weight of subcutaneous xenografts. (D) Representative IHC staining results of proliferating cell nuclear antigen (PCNA), Yes1 associated transcriptional regulator (YAP1), glucose transporter type 1 (GLUT1), hexokinase 2 (HK2), and lactate dehydrogenase A (LDHA) in subcutaneous xenografts. (E) Representative bioluminescence photograph of mice orthotopically implanted with luciferase-expressing control and LINC00941 knockdown PDAC cells, treated with gemcitabine (50 mg/kg) or not. (F) Overall survival of orthotopical PDAC mice. (G) Representative IHC staining results of PCNA, YAP1, GLUT1, HK2, and LDHA in orthotopically implanted mice. (B, C, and E) Statistical significances were calculated using two-tailed Student's t tests to compare with the NC or control group. (F) Statistical significances were calculated using log-rank Cox test. *$p < 0.05$; **$p < 0.01$; ***$p < 0.001$.

seeded in a XF96-well plate at a density of 2×10^4/well. For the glycolytic stress test (Seahorse Bioscience; catalog number [no.] 103020-100), 10 mM glucose, 1 mM oligomycin, and 50 mM 2-DG were used. For the mitochondrial stress test (Seahorse Bioscience; catalog no. 103015-100), 1 mM oligomycin, 1 mM carbonyl cyanide-*p*-trifluoromethoxyphenylhydrazone (FCCP), 0.5 mM rotenone, and 0.5 mM actinomycin A were used. Total protein was used to normalize the measurement.

Glucose uptake and lactate production

The culture medium of the cell in 6-well plates was collected to measure the glucose uptake by using a Glucose Oxidase Assay Kit (Invitrogen; catalog no. A22189) and to measure the lactate production by using a Lactate Assay Kit (BioVision Technologies; catalog no. ABIN411683) according to the manufacturers' instructions.

Western blot (WB)

For WB analyses, cells were lysed in radioimmunoprecipitation assay (RIPA) lysis buffer supplied with protease and phosphatase inhibitor cocktails (Roche). A bicinchoninic acid (BCA) assay was used to quantify protein concentration. The proteins were run on 4%–20% Tris-glycine gels (Life Technologies) and transferred to nitrocellulose membranes. Membranes were blocked with 5% w/v non-fat dry milk in Tris-buffered saline with 0.1% Tween-20. The following primary antibodies were used: anti-phospho-MST1 (Thr183)/MST2 (Thr180) (Cell Signaling Technology [CST]; #49332), anti-MST1 (CST; #14946), anti-phospho-LATS1 (Thr1079) (CST; #8654), anti-LATS1 (CST; #9153), anti-phospho-YAP (Ser127) (CST; #13008), anti-YAP1 (CST; #14074), anti-PP2A (Abcam; ab32065), and anti-β-actin (CST; #3700). Blots were imaged using horseradish peroxidase (HRP) substrate. At least two independent experiments where indicated.

ISH

ISH assay was performed to detect the expression of LINC00941 in PDAC tissues according standard protocol, as described previously.[30] The LINC00941 probe 5′-TGAATGGTCAATGTCTGGTAGTTG GACGG-3′ was tagged with double-digoxigenin (DIG). After counterstained with alkaline phosphatase (AP) substrate nitro-blue tetrazolium (NBT)-5-bromo-4-chloro-3'-indolyphosphate (BCIP) (Roche) and Nuclear Fast Red (Vector Labs, Burlingame, CA, USA), the LINC00941 level was analyzed using a microscope.

Immunofluorescence

For immunofluorescence, cells were fixed with 4% PFA at 4°C for 15 min at room temperature. Samples were blocked in 10% normal goat serum (NGS) and PBS with 0.25% Triton X-100 for 1 h at room temperature. Slides were incubated with the LINC00941 probe and MST1 antibody (CST; #14946) at 4°C overnight, following secondary antibody incubation for 2 h at room temperature. Slides were mounted with ProLong Gold Anti-Fade Reagent (Life Technologies) and imaged with a confocal microscope (Zeiss).

ChIP-quantitative PCR (qPCR)

A ChIP experiment was conducted as described previously.[38] Briefly, cross-linked chromatin and protein complexes prepared using 1% formaldehyde were sonicated into about 300 bp fragments. The soluble material was then purified by centrifugation and mixed with polyclonal antibodies against YAP1 control rabbit IgG overnight at 4°C, followed by incubation with magnetic protein G beads under reverse rotation at 4°C for 2 h. qPCR was used to analyze binding of the YAP1 to the GLUT1, HK2, and LDHA promoter. The primers were provided in the Table S2.

RIP

RIP was performed to detect the interaction of LINC000941 with MST1 via the EZ-Magna RIP Kit (Millipore, USA). Samples were prepared according to the manufacturer's instructions as previously described.[38] After the RNA was extracted, reverse transcription and qRT-PCR were performed.

IHC

IHC staining of paraffin-embedded sections was performed according to the manufacturer's instructions. After the deparaffinization, rehydration, antigen retrieval, and block, slides were incubated with inhibitor of nuclear factor kappa-B kinase α (IKKα), oligodendrocyte transcription factor 2 (OLIG2), and CD44 antigen (CD44) primary antibodies. Then slides were visualized by the standard avidin-biotinylated peroxidase complex method. Hematoxylin was used for counterstaining, and morphologic images were observed with a light microscope (Leica). Two different pathologists evaluated the immunohistological samples.

RNA pull-down assays

RNA pull-down assays were performed according to the manufacturer's protocols. Briefly, biotin-labeled RNA was transcribed with Biotin RNA Labeling Mix and T7 RNA polymerase and purified. Purified biotin-labeled RNA was then heated and annealed to form a secondary structure, mixed with cytoplasmic extract in RIP buffer for 1 h, and incubated with streptavidin agarose beads for 1 h. Finally, the beads were extracted with TRIzol reagent for qPCR analysis

Mass spectrum analysis

Mass spectrum analysis was performed according standard procedure. Briefly, the precipitations were separated by SDS-PAGE, following Coomassie blue staining. The different bands were excised from the gel and analyzed by matrix-assisted laser desorption/ionization time-of-flight/time-of-flight mass spectrometry.

Dual-luciferase reporter assay

Luciferase assays were performed as previously described;[39] cells were co-transfected with LINC000941 and firefly luciferase reporter constructs containing the transcription factor reporters in pGL3-basic vectors. Then, the cells were collected and analyzed with the luciferase reporter assay kit according to the manufacturer's instructions (Promega, Madison, WI, USA), and the results were presented as relative luciferase activities.

Animal models

The animal studies were approved by the Institutional Animal Care and Use Committee (IACUC) of Tongji University. Standard animal

care and laboratory guidelines were conducted according to the IACUC protocol. Subcutaneous xenograft was established by injecting 5×10^5 cells/mouse PDAC tumor cells into the right flank of BALB/c athymic nude mice. The length and width of the mouse tumors were measured every 5 days with calipers, and V was calculated with the following formula: $V = (\text{length} \times \text{width}^2)/2$. Orthotopic implantations of PDAC tumor cells to mouse pancreas were performed as described previously. 5×10^5 cells per 50 μL of a 30% Matrigel:70% PBS mixture were injected into the pancreatic tails of syngeneic C57BL/6J mice. Anesthetics and analgesics were used according to the local IACUC guidelines. Tumor-bearing mice were observed each 3 days until signs of sickness appeared, or animals showed distress or weight loss of more than 10%, per the local IACUC guidelines.

Human samples

This research was approved by the Ethics Committee of East Hospital Affiliated Tongji University, Tongji University School of Medicine (2020-053), and informed consent was obtained from all patients before enrolling in the research program. Biospecimens were obtained from Shanghai East Hospital Biobank. The ten PDAC specimens used for LINC00941 expression detection were freshly collected (from 2019 to 2020), which included the PET-CT results. All patients had signed, informed consent for donating their specimens to Shanghai East Hospital Biobank.

Statistical analysis

Statistical analysis was performed by using the GraphPad Prism, version 7.0 (GraphPad Software, La Jolla, CA, USA), statistical software packages. Data are presented as mean ± standard deviations unless specifically indicated otherwise. Statistical analysis of the experimental data was carried out with the two-tailed Student's t test, two-way ANOVA, and Kaplan-Meier analysis. Differences in which $p < 0.05$ were considered statistically significant. Data were collected from at least three independent experiments.

SUPPLEMENTAL INFORMATION

Supplemental information can be found online at https://doi.org/10.1016/j.omtn.2021.07.004.

ACKNOWLEDGMENTS

The Outstanding Clinical Discipline Project of Shanghai Pudong (no. PWYgy2018-02), Research Project of Shanghai Municipal Health Commission (no. 20204Y0302), and Science and Technology Commission of Shanghai Municipality (no. 20Y11912100) provided funding.

AUTHOR CONTRIBUTIONS

Conceptualization and funding acquisition, B.C.; methodology and software, W.L.; data curation and writing – original draft preparation, M.X. and R.C.; visualization and investigation, L.Y., Y.W., and X.W.; supervision, Q.Z.; software and validation, K.W.; writing – reviewing & editing, C.D.

DECLARATION OF INTERESTS

The authors declare no competing interests.

REFERENCES

1. Rahib, L., Smith, B.D., Aizenberg, R., Rosenzweig, A.B., Fleshman, J.M., and Matrisian, L.M. (2014). Projecting cancer incidence and deaths to 2030: the unexpected burden of thyroid, liver, and pancreas cancers in the United States. Cancer Res. *74*, 2913–2921.
2. Hruban, R.H., Gaida, M.M., Thompson, E., Hong, S.M., Noë, M., Brosens, L.A.A., Jongepier, M., Offerhaus, G.J.A., and Wood, L.D. (2019). Why is pancreatic cancer so deadly? The pathologist's view. J. Pathol. *248*, 131–141.
3. Siegel, R.L., Miller, K.D., and Jemal, A. (2018). Cancer statistics, 2018. CA Cancer J. Clin. *68*, 7–30.
4. Hanahan, D., and Weinberg, R.A. (2011). Hallmarks of cancer: the next generation. Cell *144*, 646–674.
5. Ryan, D.P., Hong, T.S., and Bardeesy, N. (2014). Pancreatic adenocarcinoma. N. Engl. J. Med. *371*, 2140–2141.
6. Koppenol, W.H., Bounds, P.L., and Dang, C.V. (2011). Otto Warburg's contributions to current concepts of cancer metabolism. Nat. Rev. Cancer *11*, 325–337.
7. Karasinska, J.M., Topham, J.T., Kalloger, S.E., Jang, G.H., Denroche, R.E., Culibrk, L., Williamson, L.M., Wong, H.-L., Lee, M.K.C., O'Kane, G.M., et al. (2020). Altered Gene Expression along the Glycolysis-Cholesterol Synthesis Axis Is Associated with Outcome in Pancreatic Cancer. Clin. Cancer Res. *26*, 135–146.
8. Yang, Y., Ishak Gabra, M.B., Hanse, E.A., Lowman, X.H., Tran, T.Q., Li, H., Milman, N., Liu, J., Reid, M.A., Locasale, J.W., et al. (2019). MiR-135 suppresses glycolysis and promotes pancreatic cancer cell adaptation to metabolic stress by targeting phosphofructokinase-1. Nat. Commun. *10*, 809.
9. Hu, L.-P., Zhang, X.-X., Jiang, S.-H., Tao, L.-Y., Li, Q., Zhu, L.-L., Yang, M.-W., Huo, Y.-M., Jiang, Y.-S., Tian, G.-A., et al. (2019). Targeting Purinergic Receptor P2Y2 Prevents the Growth of Pancreatic Ductal Adenocarcinoma by Inhibiting Cancer Cell Glycolysis. Clin. Cancer Res. *25*, 1318–1330.
10. Huarte, M. (2015). The emerging role of lncRNAs in cancer. Nat. Med. *21*, 1253–1261.
11. Arun, G., Diermeier, S.D., and Spector, D.L. (2018). Therapeutic Targeting of Long Non-Coding RNAs in Cancer. Trends Mol. Med. *24*, 257–277.
12. Sun, C.C., Zhu, W., Li, S.J., Hu, W., Zhang, J., Zhuo, Y., Zhang, H., Wang, J., Zhang, Y., Huang, S.X., et al. (2020). FOXC1-mediated LINC00301 facilitates tumor progression and triggers an immune-suppressing microenvironment in non-small cell lung cancer by regulating the HIF1α pathway. Genome Med. *12*, 77.
13. Yang, P., Li, J., Peng, C., Tan, Y., Chen, R., Peng, W., Gu, Q., Zhou, J., Wang, L., Tang, J., et al. (2020). TCONS_00012883 promotes proliferation and metastasis via DDX3/YY1/MMP1/PI3K-AKT axis in colorectal cancer. Clin. Transl. Med. *10*, e211.
14. Shi, Q., Li, Y., Li, S., Jin, L., Lai, H., Wu, Y., Cai, Z., Zhu, M., Li, Q., Li, Y., et al. (2020). LncRNA DILA1 inhibits Cyclin D1 degradation and contributes to tamoxifen resistance in breast cancer. Nat. Commun. *11*, 5513.
15. Zhuang, L., Xia, W., Chen, D., Ye, Y., Hu, T., Li, S., and Hou, M. (2020). Exosomal LncRNA-NEAT1 derived from MIF-treated mesenchymal stem cells protected against doxorubicin-induced cardiac senescence through sponging miR-221-3p. J. Nanobiotechnology *18*, 157.
16. Zhou, C., Yi, C., Yi, Y., Qin, W., Yan, Y., Dong, X., Zhang, X., Huang, Y., Zhang, R., Wei, J., et al. (2020). LncRNA PVT1 promotes gemcitabine resistance of pancreatic cancer via activating Wnt/β-catenin and autophagy pathway through modulating the miR-619-5p/Pygo2 and miR-619-5p/ATG14 axes. Mol. Cancer *19*, 118.
17. Li, N., Yang, G., Luo, L., Ling, L., Wang, X., Shi, L., Lan, J., Jia, X., Zhang, Q., Long, Z., et al. (2020). THAP9-AS1lncRNA Promotes Pancreatic Ductal Adenocarcinoma Growth and Leads to a Poor Clinical Outcome via Sponging miR-484 and Interacting with YAP. Clin. Cancer Res. *26*, 1736–1748.
18. Xiong, G., Liu, C., Yang, G., Feng, M., Xu, J., Zhao, F., You, L., Zhou, L., Zheng, L., Hu, Y., et al. (2019). Long noncoding RNA GSTM3TV2 upregulates LAT2 and OLR1 by competitively sponging let-7 to promote gemcitabine resistance in pancreatic cancer. J. Hematol. Oncol. *12*, 97.

19. Sun, R.F., Zhao, C.Y., Chen, S., Yu, W., Zhou, M.M., and Gao, C.R. (2021). Androgen Receptor Stimulates Hexokinase 2 and Induces Glycolysis by PKA/CREB Signaling in Hepatocellular Carcinoma. Dig. Dis. Sci. *66*, 802–813.

20. Wang, L., Sun, J., Gao, P., Su, K., Wu, H., Li, J., and Lou, W. (2019). Wnt1-inducible signaling protein 1 regulates laryngeal squamous cell carcinoma glycolysis and chemoresistance via the YAP1/TEAD1/GLUT1 pathway. J. Cell. Physiol. Published online February 25, 2019. https://doi.org/10.1002/jcp.28253.

21. Jiao, L., Wang, S., Zheng, Y., Wang, N., Yang, B., Wang, D., Yang, D., Mei, W., Zhao, Z., and Wang, Z. (2019). Betulinic acid suppresses breast cancer aerobic glycolysis via caveolin-1/NF-κB/c-Myc pathway. Biochem. Pharmacol. *161*, 149–162.

22. Kuwabara, S., Yamaki, M., Yu, H., and Itoh, M. (2018). Notch signaling regulates the expression of glycolysis-related genes in a context-dependent manner during embryonic development. Biochem. Biophys. Res. Commun. *503*, 803–808.

23. Oginuma, M., Harima, Y., Tarazona, O.A., Diaz-Cuadros, M., Michaut, A., Ishitani, T., Xiong, F., and Pourquié, O. (2020). Intracellular pH controls WNT downstream of glycolysis in amniote embryos. Nature *584*, 98–101.

24. Tang, Y., Fang, G., Guo, F., Zhang, H., Chen, X., An, L., Chen, M., Zhou, L., Wang, W., Ye, T., et al. (2020). Selective Inhibition of STRN3-Containing PP2A Phosphatase Restores Hippo Tumor-Suppressor Activity in Gastric Cancer. Cancer Cell *38*, 115–128.e9.

25. Yan, X., Zhang, D., Wu, W., Wu, S., Qian, J., Hao, Y., Yan, F., Zhu, P., Wu, J., Huang, G., et al. (2017). Mesenchymal stem cells promote hepatocarcinogenesis via lncRNA–MUF interaction with ANXA2 and miR-34a. Cancer Res. *77*, 6704–6716.

26. Liu, H., Wu, N., Zhang, Z., Zhong, X., Zhang, H., Guo, H., Nie, Y., and Liu, Y. (2019). Long Non-coding RNA *LINC00941* as a Potential Biomarker Promotes the Proliferation and Metastasis of Gastric Cancer. Front. Genet. *10*, 5.

27. Ai, Y., Wu, S., Zou, C., and Wei, H. (2020). LINC00941 promotes oral squamous cell carcinoma progression via activating CAPRIN2 and canonical WNT/β-catenin signaling pathway. J. Cell. Mol. Med. *24*, 10512–10524.

28. Wang, L., Zhao, H., Xu, Y., Li, J., Deng, C., Deng, Y., Bai, J., Li, X., Xiao, Y., and Zhang, Y. (2019). Systematic identification of lincRNA-based prognostic biomarkers by integrating lincRNA expression and copy number variation in lung adenocarcinoma. Int. J. Cancer *144*, 1723–1734.

29. Gugnoni, M., Manicardi, V., Torricelli, F., Sauta, E., Bellazzi, R., Manzotti, G., Vitale, E., de Biase, D., Piana, S., and Ciarrocchi, A. (2021). Linc00941 Is a Novel Transforming Growth Factor β Target That Primes Papillary Thyroid Cancer Metastatic Behavior by Regulating the Expression of Cadherin 6. Thyroid *31*, 247–263.

30. Wu, N., Jiang, M., Liu, H., Chu, Y., Wang, D., Cao, J., Wang, Z., Xie, X., Han, Y., and Xu, B. (2021). LINC00941 promotes CRC metastasis through preventing SMAD4 protein degradation and activating the TGF-β/SMAD2/3 signaling pathway. Cell Death Differ. *28*, 219–232.

31. Yu, F.X., Zhao, B., and Guan, K.L. (2015). Hippo Pathway in Organ Size Control, Tissue Homeostasis, and Cancer. Cell *163*, 811–828.

32. Zheng, X., Han, H., Liu, G.P., Ma, Y.X., Pan, R.L., Sang, L.J., Li, R.H., Yang, L.J., Marks, J.R., Wang, W., and Lin, A. (2017). LncRNA wires up Hippo and Hedgehog signaling to reprogramme glucose metabolism. EMBO J. *36*, 3325–3335.

33. Zhang, X., Li, Y., Ma, Y., Yang, L., Wang, T., Meng, X., Zong, Z., Sun, X., Hua, X., and Li, H. (2018). Yes-associated protein (YAP) binds to HIF-1α and sustains HIF-1α protein stability to promote hepatocellular carcinoma cell glycolysis under hypoxic stress. J. Exp. Clin. Cancer Res. *37*, 216.

34. Ni, W., Zhang, Y., Zhan, Z., Ye, F., Liang, Y., Huang, J., Chen, K., Chen, L., and Ding, Y. (2017). A novel lncRNA uc.134 represses hepatocellular carcinoma progression by inhibiting CUL4A-mediated ubiquitination of LATS1. J. Hematol. Oncol. *10*, 91.

35. Wu, D.-M., Wang, S., Wen, X., Han, X.-R., Wang, Y.-J., Shen, M., Fan, S.-H., Zhang, Z.-F., Shan, Q., Li, M.-Q., et al. (2018). LncRNA SNHG15 acts as a ceRNA to regulate YAP1-Hippo signaling pathway by sponging miR-200a-3p in papillary thyroid carcinoma. Cell Death Dis. *9*, 947.

36. Li, C., Wang, S., Xing, Z., Lin, A., Liang, K., Song, J., Hu, Q., Yao, J., Chen, Z., Park, P.K., et al. (2017). A ROR1-HER3-lncRNA signalling axis modulates the Hippo-YAP pathway to regulate bone metastasis. Nat. Cell Biol. *19*, 106–119.

38. Luo, H., Zhu, G., Xu, J., Lai, Q., Yan, B., Guo, Y., Fung, T.K., Zeisig, B.B., Cui, Y., Zha, J., et al. (2019). HOTTIP lncRNA Promotes Hematopoietic Stem Cell Self-Renewal Leading to AML-like Disease in Mice. Cancer Cell *36*, 645–659.e8.

39. Wei, Y., Lu, C., Zhou, P., Zhao, L., Lyu, X., Yin, J., Shi, Z., and You, Y. (2021). EIF4A3-induced circular RNA ASAP1 promotes tumorigenesis and temozolomide resistance of glioblastoma via NRAS/MEK1/ERK1-2 signaling. Neuro Oncol. *23*, 611–624.